Electronic Supplementary Material (ESI) for CrystEngComm.
This journal is © The Royal Society of Chemistry 2023

The Introduction of a Base Component to Porous Organic Salts and Their CO_2 Storage Capability

Takahiro Ami,[a†] Kouki Oka,[a†] Keiho Tsuchiya,[a] Wataru Kosaka,[bc] Hitoshi Miyasaka,[bc] and Norimitsu Tohnai*[a]

a. Department of Applied Chemistry and Center for Future Innovation (CFi), Graduate School of Engineering, Osaka University, 2-1 Yamadaoka, Suita, Osaka 565-0871, Japan.
Email: tohnai@chem.eng.osaka-u.ac.jp (Norimitsu Tohnai)

b. Institute for Materials Research, Tohoku University, 2-1-1 Katahira, Aoba-ku, Sendai 980-8577, Japan.

c. Department of Chemistry, Graduate School of Science, Tohoku University, 6-3 Aramaki-Aza-Aoba, Aoba-ku, Sendai 980-8578, Japan

†T.A and K.O. contributed equally to this work.

Experimental Sections

Materials.

Hypophosphorous Acid (50 wt. % in H_2O) was purchased from Sigma-Aldrich Co. LCC. Bromine, 4-bromobenzenesulfonyl chloride, 5-bromopyrimidine, 1,4-isoamyl nitrate, methyltri-*n*-octylammonium chloride, pararosaniline hydrochloride, thionyl chloride, trifluoroacetic acid, triphenylmethylamine, and trityl chloride were purchased from Tokyo Chemical Industry Co, ltd. Other chemicals were purchased from FUJIFILM Wako Pure Chemical Corporation.

Measurements.

Proton and carbon nuclear magnetic resonance (^{1}H NMR and ^{13}C NMR) spectra were recorded by a JEOL 400 JJYH (400 MHz) spectrometer with chemical shifts downfield from tetramethylsilane as the internal standard. Thermal analyses were performed with a Rigaku TG8120 at a heating rate of 3 °C min^{-1} under nitrogen. Gas adsorption measurements were performed on BELSORP-max from MicrotracBEL, Japan. The N_2 and O_2 adsorption measurements were demonstrated at 77 K. The CO_2 adsorption measurement was demonstrated at

195 K. Before all measurements, the samples were dried under reduced pressure and 363 K for 2 h.

The X-ray diffraction data of the organic salts was collected on a two-dimensional X-ray detector (PILATUS 200 K/R) equipped in Rigaku XtaLAB PRO diffractometer using thin multi-layer mirror monochromated Cu-Kα radiation (λ = 1.54187 Å). The cell refinements were performed with CrysAlisPro a software 1.171.39.5. SHELXT was used for the structure solution of the crystals. All calculations were performed with the observed reflections [I>2σ(I)] with the program CrystalStructure crystallographic software packages, except for refinement which was performed by SHELXL. All non-hydrogen atoms, except for highly disordered solvent molecules accommodated in voids, were refined with anisotropic displacement parameters, and hydrogen atoms were placed in idealized positions and refined as rigid atoms with the relative isotropic displacement parameters. SQUEEZE function equipped in the PLATON program was used to remove severely disordered solvent molecules in the voids for ***d*-POSs**.

Powder X-ray diffraction (**PXRD**) was performed with a Rigaku Ultima IV using graphite monochromatized Cu-Kα radiation (λ = 1.54187 Å) at 25°C.

Synthesis of diphenyl(pyrimidine-5-yl)methylamine (DPPMA).

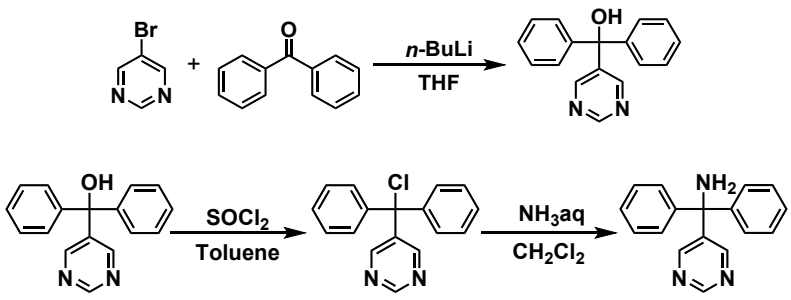

Scheme S1. Synthesis of diphenyl(pyrimidine-5-yl)methylamine.

5-Bromopyrimidine (4.00 g, 25.1 mmol) was added to anhydrous THF (60 mL) under nitrogen, and then *n*-BuLi (1.6 M in hexane, 16 mL) was dropped into the mixture at -78°C. The mixture was stirred at -78°C for 30 min. Then, anhydrous THF (20 mL) containing benzophenone (4.25 g, 22.6 mmol) was dropped into the mixture. The mixture was stirred at -78°C overnight. Then, the reaction was quenched by adding saturated aqueous ammonium chloride solution. The mixture was extracted with ethyl acetate/water, and then was purified using column chromatography on silica gel with hexane/ethyl acetate (1/1) as eluents. The residue was recrystallized in hexane to give a white solid (1.21 g).

Then, the solid (1.21 g) and thionyl chloride (8.0 mL, 110 mmol) were added to dichloromethane (30 mL). The mixture was stirred at 25°C for 8 h. After the evaporation of the solvent, the residue and dichloromethane (30 mL) were added

to aqueous ammonia solution (28 wt. %, 30 mL) containing ammonium chloride (2.02 g, 37.8 mmol) at 25°C. The mixture was stirred at 25°C overnight. After the reaction, the mixture was extracted with dichloromethane/water, and then was purified using column chromatography on silica gel with ethylacetate as an eluent to give a white solid. The solid was characterized as **DPPMA** (0.897 mg, 15 %), as follows (Figures S13 and S14): ^{1}H-NMR (400 MHz, dimethyl sulfoxide-d_6, δ): 7.42 (d, J = 8.8 Hz, 6H), 7.12 (d, J = 8.4 Hz, 6H), 2.21 (br, 2H); ^{13}C NMR (400 MHz, dimethyl sulfoxide-d_6, δ): 146.7, 131.2, 129.7, 121.2, 65.4.

Preparation of tetrakis(4-bromophenyl)methane

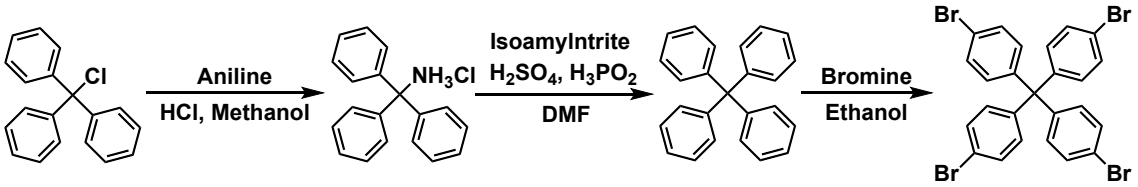

Scheme S2. Synthesis of tetrakis(4-bromophenyl)methane.

We synthesized tetrakis(4-bromophenyl)methane following the previous report[1, 2]. Trityl chloride (10.5 g, 37.5 mmol) was added to aniline (9.5 mL, 100 mmol). The mixture was stirred at 200°C until the mixture turned into a violet solid. MeOH (35 mL) and HCl (2M, 45 mL) were then added to the mixture. The mixture was stirred overnight at 90°C. After the reaction, the mixture was filtered and washed with water. After the evaporation of the solvent, sulfuric acid (10.5 mL) and isoamyl nitrite (6.16 g, 52.6 mmol) was added to the residue at 0°C. The mixture was stirred for 1 h at 0°C, and hypophosphorous acid (50 wt. % in water, 19 mL) was then dropped into the mixture. The mixture was stirred for 1.5 h at 50°C. After the reaction, the mixture was filtered and washed with ethanol and water to give a tetraphenylmethane (9.52 g, 79 %).

Bromine (20.0 g, 125 mmol) was dropped to the tetraphenylmethane (2.00 g, 6.24 mmol). The mixture was stirred for 20 min at 25°C and ethanol (100 mL) was then

added to the mixture. The mixture was stirred for 4 h at 0°C. After the reaction, the reaction was quenched by adding aqueous $N_2S_2O_5$ solution, and then the mixture was filtered and washed with water. The filter cake was dried and purified using reflux with ethyl acetate to give a yellow solid. The solid was characterized as tetrakis(4-bromophenyl)methane (2.90 g, 73 %): ^{1}H-NMR (400 MHz, dimethyl sulfoxide-d_6, δ): 7.53 (d, J = 9.2 Hz, 8H), 7.06 (d, J = 8.8 Hz, 8H).

Preparation of neopentyl 4-(4,4,5,5-tetramethyl-1,3,2-dioxa borolan-2-yl)benzenesulfonate.

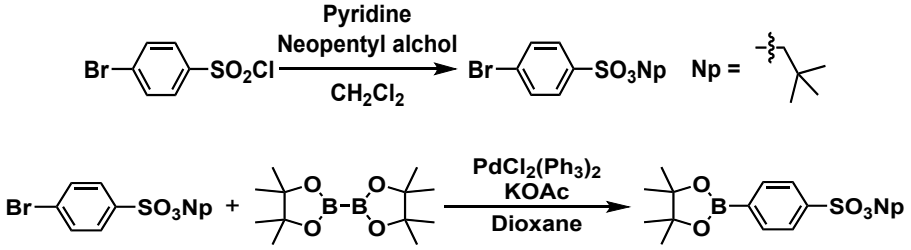

Scheme S3. Synthesis of neopentyl 4-(4,4,5,5-tetramethyl-1,3,2-dioxa borolan-2-yl)benzenesulfonate.

We synthesized neopentyl 4-(4,4,5,5-tetramethyl-1,3,2-dioxa borolan-2-yl)benzenesulfonate following the previous report[3]. Pyridine (19 mL, 240 mmol) was added to 4-bromobenzenesulfonyl chloride (50.4 g, 199 mmol), and dichloromethane (50 mL) containing neopentyl alcohol (20.8 g, 236 mmol) was then dropped into the mixture at 0°C. The mixture was stirred for 2 h at 0°C, and then it was stirred overnight at 25°C. After the evaporation of pyridine, the mixture was extracted with dichloromethane/aqueous HCl solution (0.5M), dichloromethane/sodium bicarbonate, and dichloromethane/water, and then purified using recrystallization with hexane to give neopentyl 4-bromobenzenesulfonate (39.8 g, 65 %).

Then, neopentyl 4-bromobenzenesulfonate (5.05 g, 16.3 mmol) and bis(pinacolate)diboron (5.05 g, 19.5 mmol), $PdCl_2(PPh_3)_2$ (240 mg, 0.325 mmol), potassium acetate (4.77 g, 48.6 mmol) were added to dioxane (115 mL) under nitrogen. The mixture was stirred overnight at 120°C. After the reaction, the mixture was extracted with ethyl acetate/water, and then purified using column chromatography on silica gel with ethyl acetate/hexane (1/10) as eluents and recrystallization with 2-propanol to give a white solid. The solid was characterized as neopentyl 4-(4,4,5,5-tetramethyl-1,3,2-dioxa borolan-2-yl)benzenesulfonate (4.81 g, 80 %), : ^{1}H-NMR (400 MHz, chloroform-d_1, δ): 7.97 (d, J = 8.8 Hz, 2H), 7.88 (d, J = 8.4 Hz, 2H), 3.66 (s, 2H), 1.36 (s, 12H), 0.89 (s, 9H).

Synthesis of 4',4''',4'''',4'''''-methanetetrayltetrakis(([1,1'-biphenyl]-4-sulfonic acid)) (MTBPS).

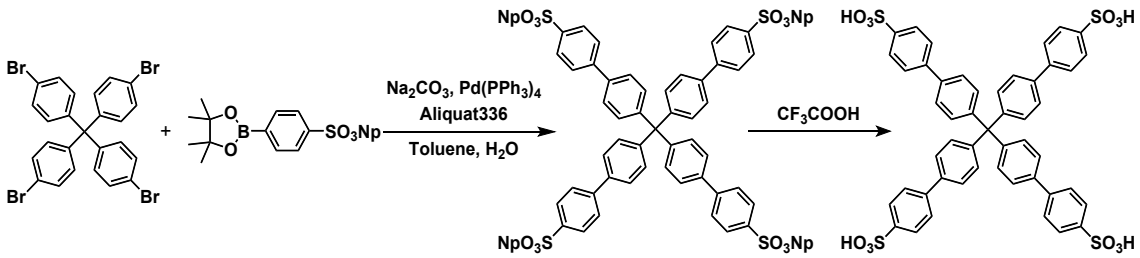

Scheme S4. Synthesis of 4',4''',4'''',4'''''-methanetetrayltetrakis(([1,1'-biphenyl]-4-sulfonic acid)) (**MTBPS**).

4-(4,4,5,5-Tetramethyl-1,3,2-dioxa borolan-2-yl)benzenesulfonate (2.28 g, 5.78 mmol) and tetrakis(4-bromophenyl)methane (735 mg, 1.16 mmol), sodium carbonate (1.23 g, 11.6 mmol), $Pd(PPh_3)_3$ (135 mg, 0.116 mmol), aliquat336 (137 mg) were added to toluene (26 mL), H_2O (13 mL) and ethanol (2.6 mL) under nitrogen. The mixture was stirred overnight at 90°C. After the evaporation of the solvent, the residue was extracted with chloroform/water and then purified using reflux with ethyl acetate and recrystallization with chloroform to give tetraneopentyl 4',4''',4'''',4'''''-methanetetrayltetrakis([1,1'-biphenyl]-4-sulfonate) (1.32 g, 80 %).

Then, tetraneopentyl 4',4''',4'''',4'''''-methanetetrayltetrakis([1,1'-biphenyl]-4-sulfonate) (470 mg, 0.393 mmol) were added to trifluoroacetic acid (80 mL). The

mixture was stirred overnight at 70°C. After the evaporation of the solvent, the residue was purified using reflux with ethyl acetate to give a pale pink solid. The solid was characterized as **MTBPS** (243 mg, 67 %): ^{1}H-NMR (400 MHz, DMSO-$d_{6,}$ δ): 7.27 (d, J = 8.4 Hz, 8H), 7.22 (s, 16H), 6.95 (d, J = 8.4 Hz, 8H); ^{13}C NMR (400 MHz, dimethyl sulfoxide -d_6, δ): 147.2, 145.5, 139.4, 137.1, 130.9, 126.1, 126.0, 125.8, 63.6.

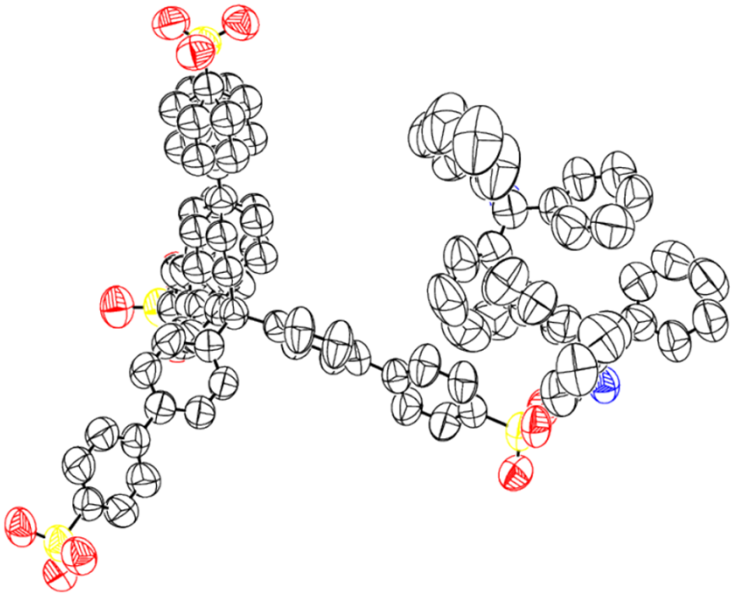

Figure S1. ORTEP drawing of the crystal structure of **TPMA/MTBPS**.

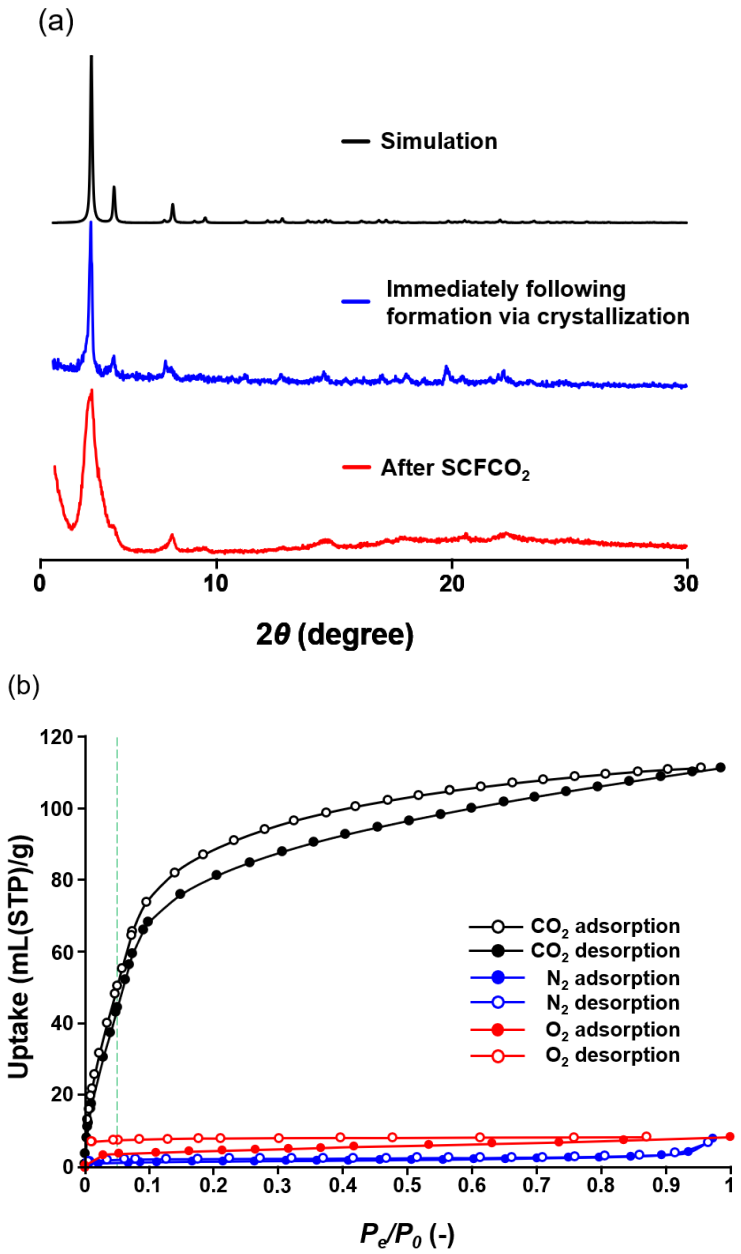

Figure S2. (a) Powder X-ray diffraction (**PXRD**) patterns of **TPMA/MTBPS**, simulation (black), immediately following formation via crystallization (blue), after conducting the supercritical fluid carbon dioxide (**SCFCO$_2$**) process for 5 h (red). (b) Gas adsorption/desorption isotherms of **TPMA/MTBPS** in the cases of nitrogen (N_2, 77 K), oxygen (O_2, 77 K), and carbon dioxide (CO_2, 195 K). P_e denotes the pressure at gas adsorption and P_0 is the condensation pressure of the adsorbate at the measurement temperature. Green line is P_e/P_0 = 0.05.

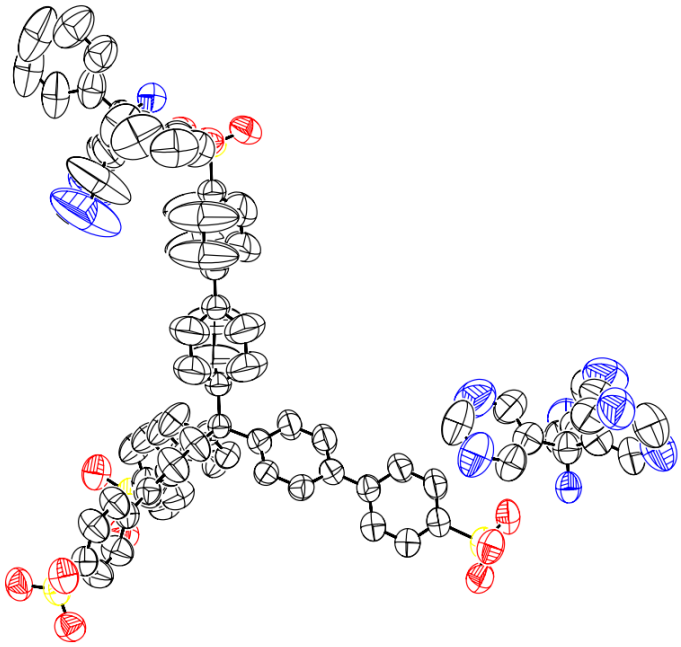

Figure S3. ORTEP drawing of the crystal structure of **DPPMA/MTBPS**.

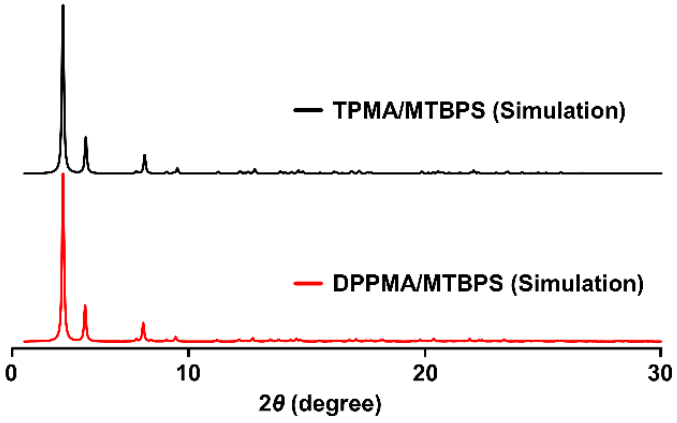

Figure S4. Simulation of powder X-ray diffraction (**PXRD**) patterns of **TPMA/MTBPS** (black) and **DPPMA/MTBPS** (red).

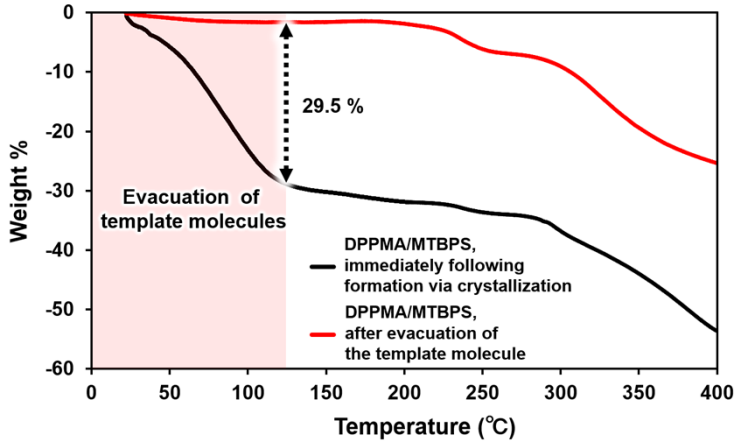

Figure S5. Thermogravimetric analysis (**TGA**) data of **DPPMA/MTBPS** immediately following formation via crystallization (black line), **DPPMA/MTBPS** after evacuation of the template molecule (red line).

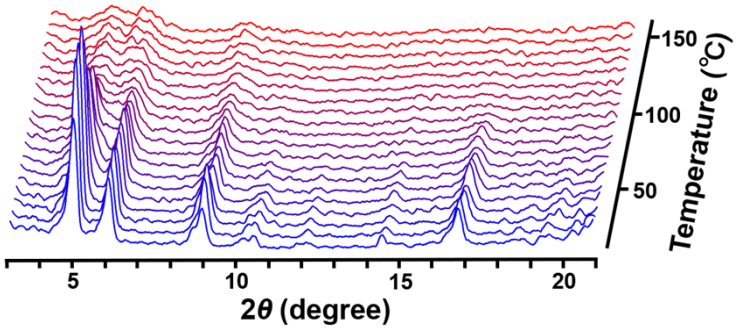

Figure S6. Variable powder X-ray diffraction (**VT-PXRD**) patterns of **DPPMA/MTBPS**.

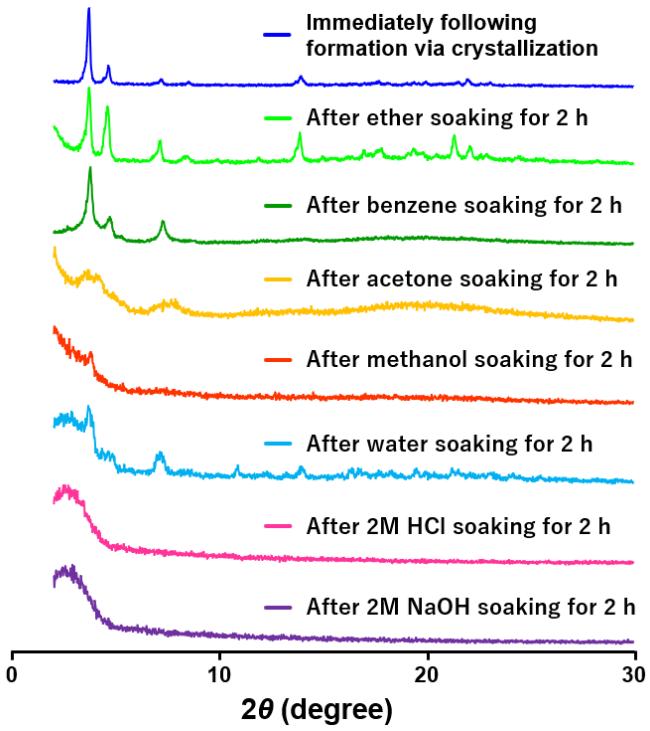

Figure S7. Powder X-ray diffraction (**PXRD**) patterns showing the chemical stability of **DPPMA/MTBPS**, immediately following formation via crystallization (blue line), after ether soaking for 2 h (light green line), after benzene soaking for 2 h (green line), after acetone soaking for 2 h (yellow line), after methanol soaking for 2 h (orange line), after water soaking for 2 h (light blue line), after 2M HCl soaking for 2 h (pink line), after 2M NaOH soaking for 2 h (purple line).

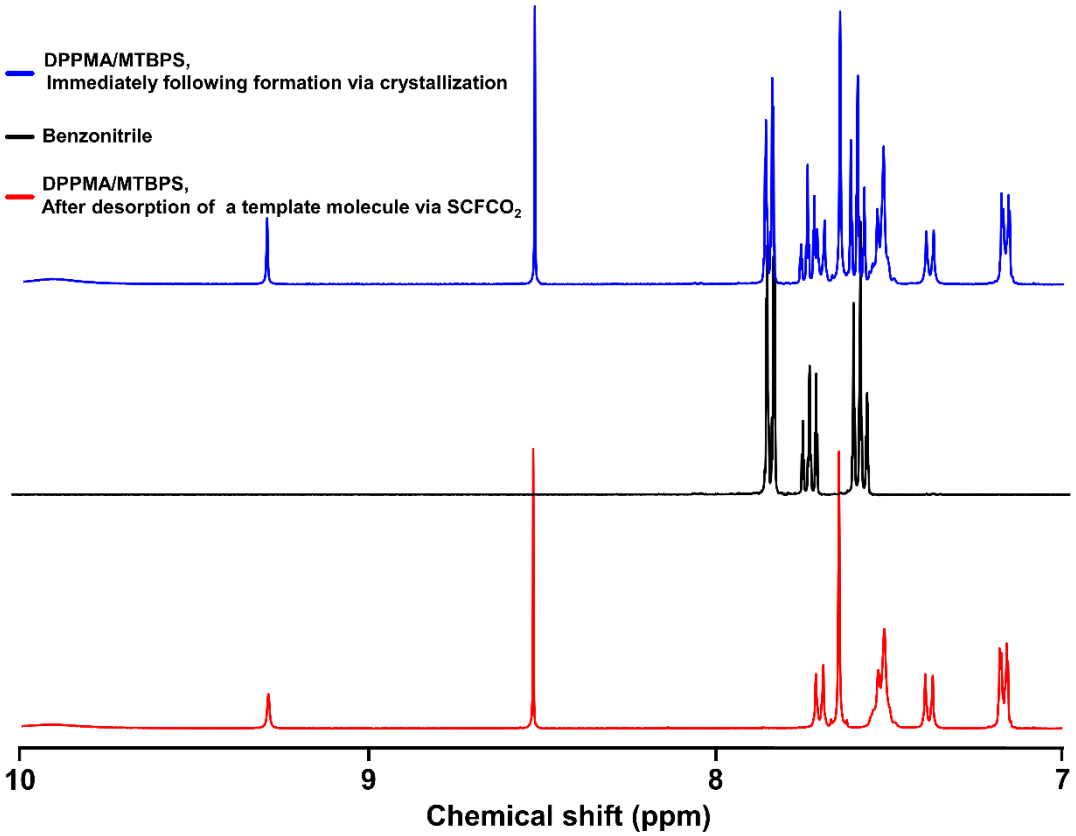

Figure S8. 400 MHz ^{1}H NMR spectra (dimethyl sulfoxide-d_6) of **DPPMA/MTBPS** immediately following formation via crystallization (blue) and after evacuation of the template molecule (red) by the supercritical fluid carbon dioxide (**$SCFCO_2$**), benzonitrile (black) which is the guest molecule for **DPPMA/MTBPS**. This figure indicated the complete progress of the evacuation of the template molecule by **$SCFCO_2$**.

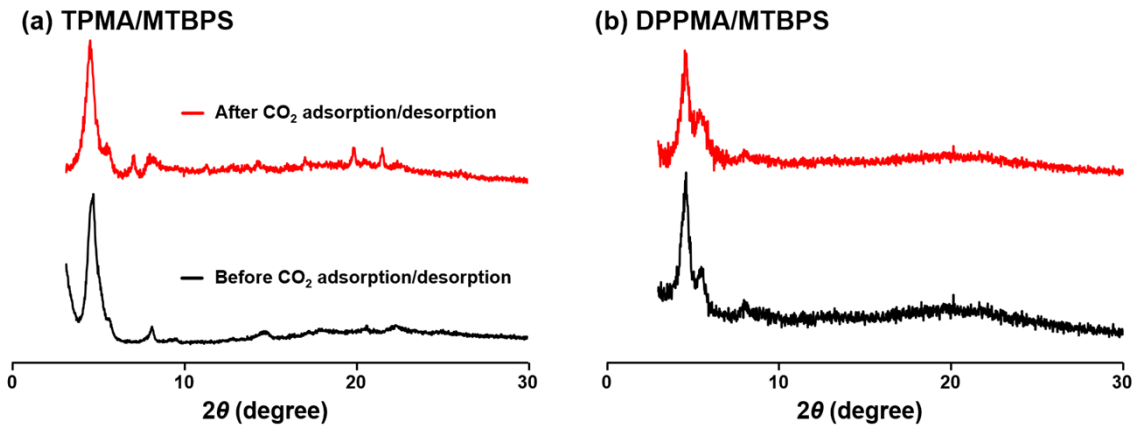

Figure S9. Powder X-ray diffraction (PXRD) patterns of **TPMA/MTBPS** and **DPPMA/MTBPS**. Before CO_2 adsorption/desorption measurement (black), after CO_2 adsorption/desorption measurement (red).

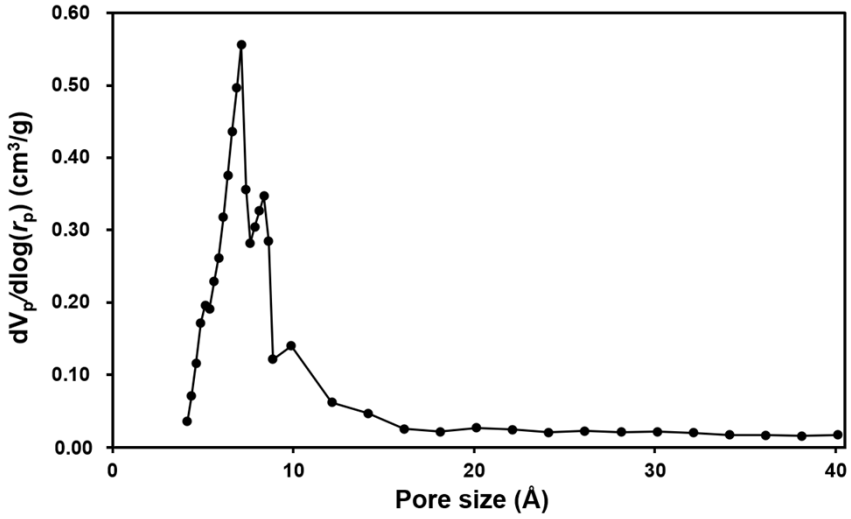

Figure S10. Pore size distribution plots of **DPPMA/MTBPS** based on the CO_2 adsorption isotherm obtained using **SF** model.

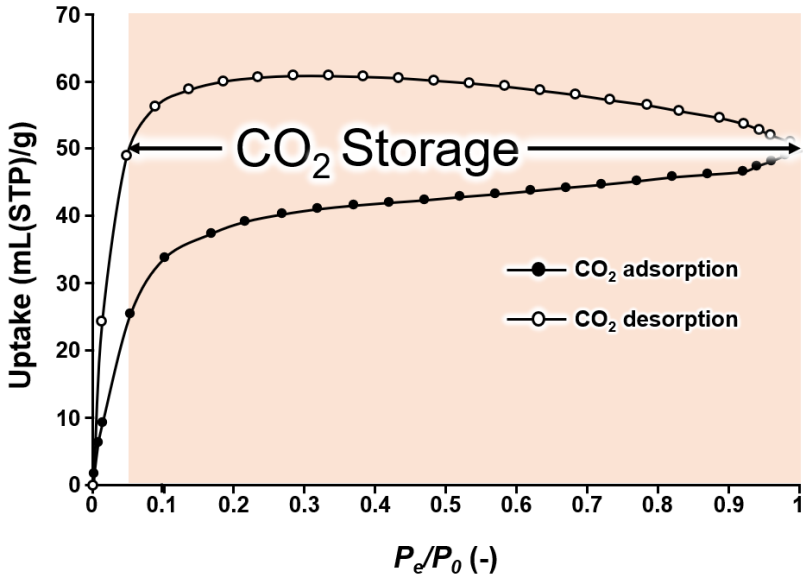

Figure S11. Gas adsorption/desorption isotherms of **DPPMA/MTBPS** in the cases of carbon dioxide (CO_2, 195 K). P_e denotes the pressure at gas adsorption and P_0 is the condensation pressure of the adsorbate at the measurement temperature. The amount of CO_2 adsorption of **DPPMA/MTBPS** reaches a maximum value at P_e/P_0 = 0.2 in the desorption isotherm which is common in porous structures with complicated micropores such as **MOFs** because of the extremely slow diffusion rate of the adsorbent in their void.[4] Although we repeatedly measured CO_2 adsorption/desorption experiments multiple times under stricter equilibrium conditions, the isotherm showed the same results.

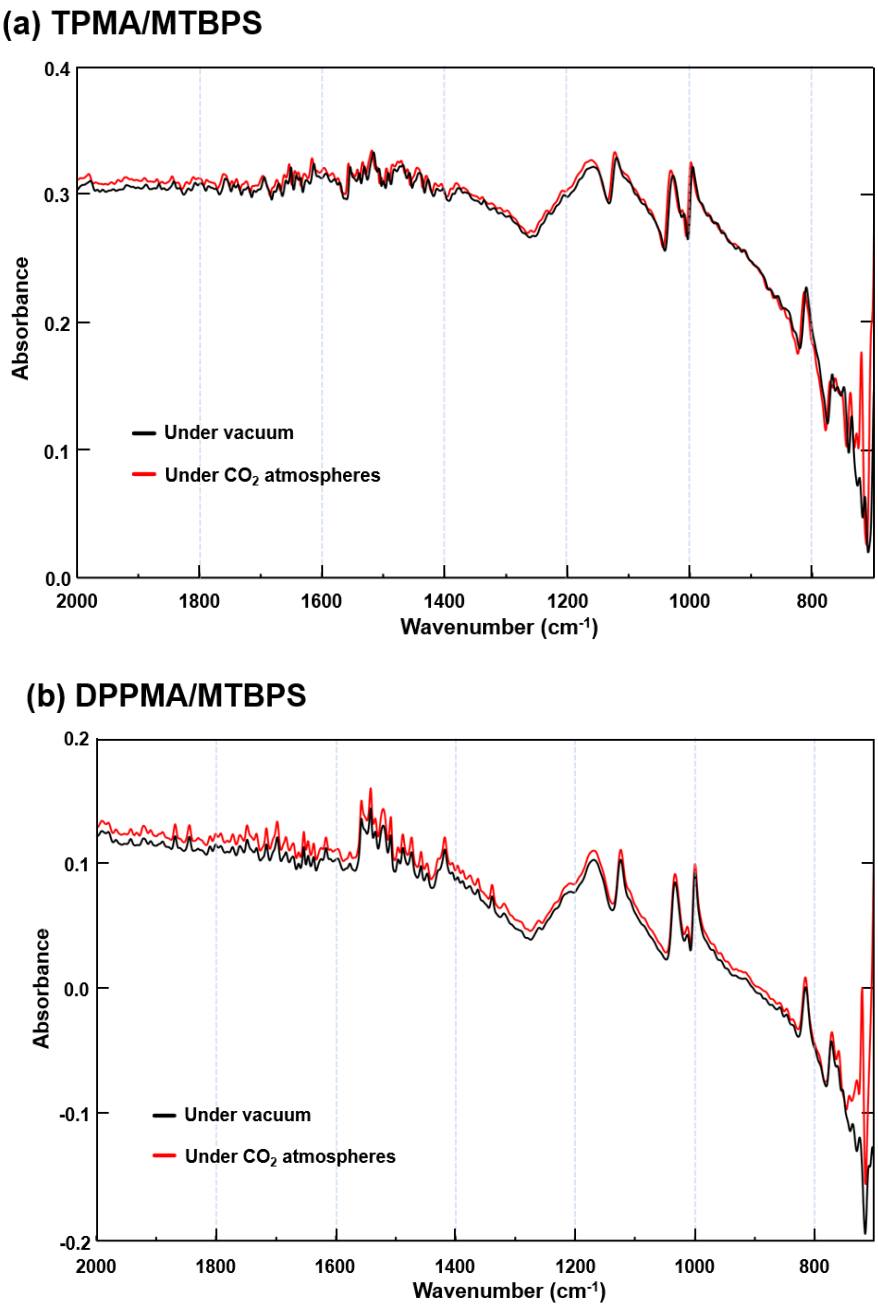

Figure S12. Fourier transform infrared (**FT-IR**) spectra of (a) **TPMA/MTBPS** and (b) **DPPMA/MTBPS**, which are measured under vacuum (black line) and CO_2 atmospheres (red line).

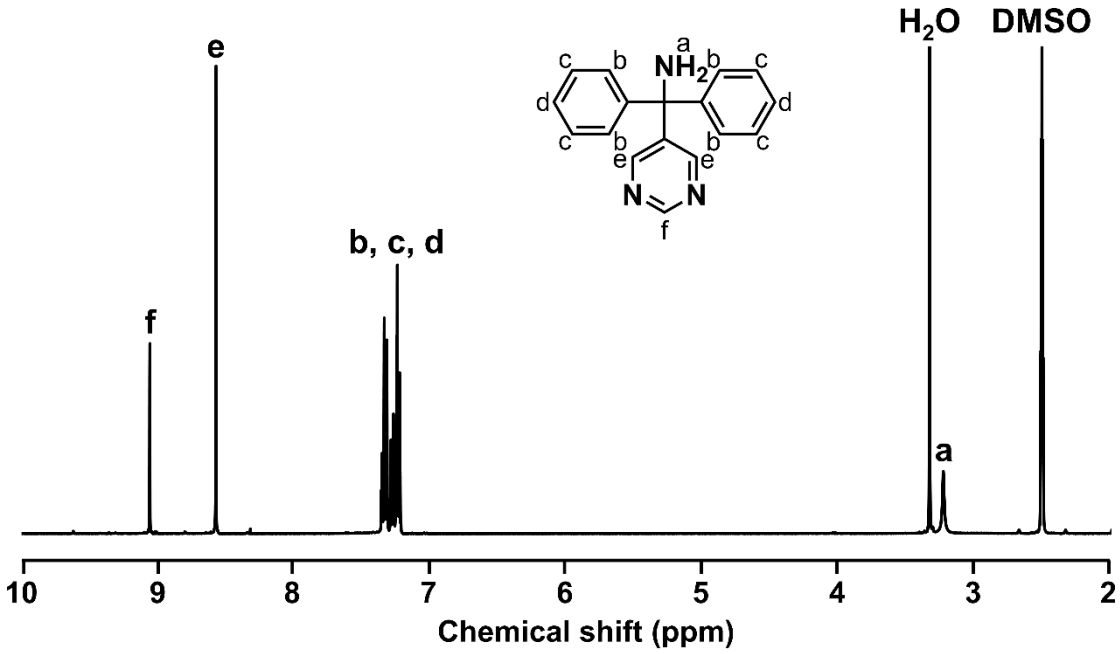

Figure S13. 400 MHz ^{1}H NMR spectrum (dimethyl sulfoxide-d_6) of diphenyl(pyrimidine-5-yl)methylamine (**DPPMA**).

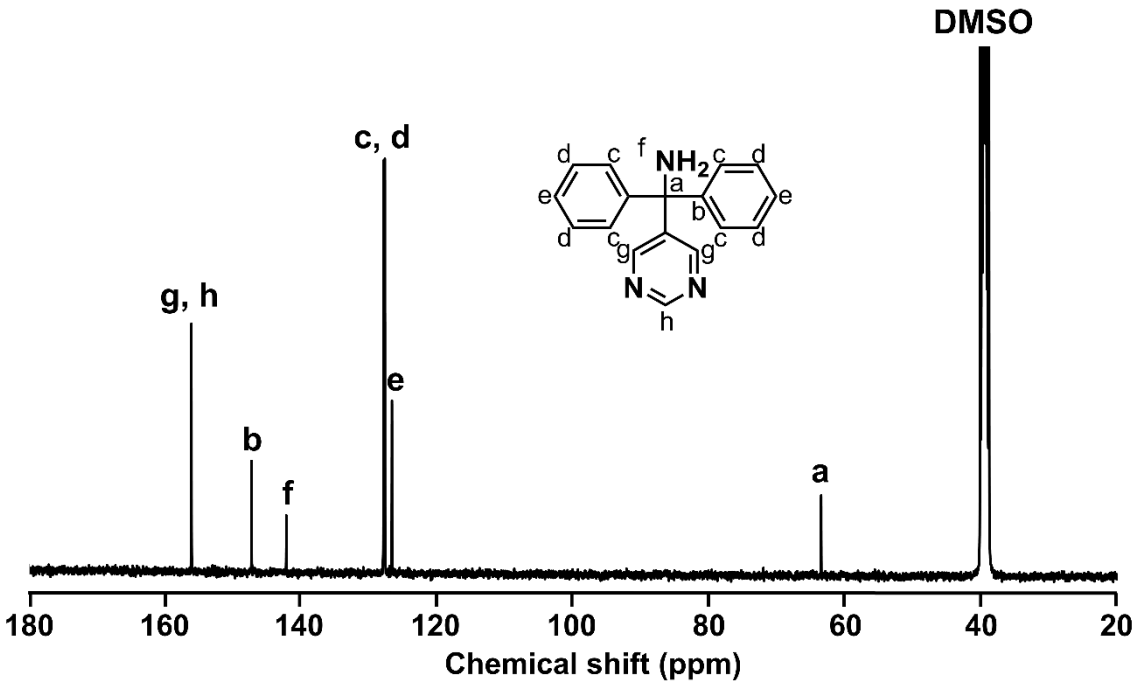

Figure S14. 400 MHz ^{13}C NMR spectrum (dimethyl sulfoxide-d_6) of diphenyl(pyrimidine-5-yl)methylamine (**DPPMA**).

Table S1. Crystallographic Parameters of ***d*-POSs**. In the crystal structure of **DPPMA/MTBPS**, a **DPPMA** is placed on the three-fold axis, therefore some benzene rings are replaced by pyrimidine rings.

	TPMA/MTBPS	**DPPMA/MTBPS**
formula	$C_{164}H_{161}N_{13}O_{18}S_4$	$C_{162}\ H_{165}\ N_{21}\ O_{18}\ S_4$
fw	2730.29	2822.38
crystal system	trigonal	trigonal
space group	*R*-3	*R* -3*c*
a [Å]	21.8052(5)	21.9765(4)
b [Å]	21.8052(5)	21.9765(4)
c [Å]	57.148(2)	114.166(2)
α [deg]	90	90
β [deg]	90	90
γ [deg]	120	120
V [Å^3]	23531.6(11)	47751(2)
Z	6	12
T [K]	203	213
R_1 (I>2σ(I))	0.0755	0.1050
Rw (all data)	0.1852	0.3460
CCDC no.	2152672	2160329

Table S2. The porosity of ***d*-POSs** (calculated by PLATON/VOID routine) and BET surface area of ***d*-POSs** based on CO_2 adsorption measurement.

	TPMA/MTBPS	**DPPMA/MTBPS**
Porosity of the void [%]	40.7	43.8
CO_2 BET surface area [m^2/g]	376	192

Table S3. The porosity (calculated by PLATON/VOID routine) and the number of interpenetration of diamond networks.of previously reported ***d*-POSs** and organic porous structures with diamond networks.

	Porosity of the void [%]	Number of interpenetration of diamond networks.	Ref
1-Pys-TPMA-TMB	22.0	2	5
2AS- TPMA-TMB	23.1	3	6
2AS- TPMA-TCB	28.4	3	6
SBDS-TPMA-CT	22.7	4	7
TPMA/MTBPS	40.7	2	8
TPMA-F/MTBPS	41.4	2	8
TPMA-Cl/MTBPS	32.5	2	8
TPMA-Br/MTBPS	31.7	2	8
TPM-I/MTBPS	26.4	2	8
Compound 1	30.1	8	9
1,3,5,7-tetrakis (4-phosphonophenyl)adamantane	24.4	4	10
Compound 9	nonporous	10	11
NPN-1	36.3	4	12
NPN-2	39.2	4	12
NPN-3	34.2	6	12
DPPMA/MTBPS	**43.8**	**2**	**This work**

References

1. A. Sickinger and S. Mecking, *Macromolecules*, 2021, **54**, 5267-5277.
2. C. Klumpen, M. Breunig, T. Homburg, N. Stock and J. Senker, *Chem. Mater.*, 2016, **28**, 5461-5470.
3. W. Qu, X. Zhu, J. Chen, L. Niu, D. Liang, X. Fan, Z. Shen and Q. Zhou, *Macromolecules*, 2014, **47**, 2727-2735.
4. J. Ethiraj, S. Palla and H. Reinsch, *Microporous and Mesoporous Materials*, 2020, **294**, 109867.
5. A. Yamamoto, S. Uehara, T. Hamada, M. Miyata, I. Hisaki and N. Tohnai, *Cryst. Growth Des.*, 2012, **12**, 4600-4606.
6. A. Yamamoto, T. Hamada, I. Hisaki, M. Miyata and N. Tohnai, *Angew. Chem. Int. Ed.*, 2013, **52**, 1709-1712.
7. A. Yamamoto, T. Hirukawa, I. Hisaki, M. Miyata and N. Tohnai, *Tetrahedron Lett.*, 2013, **54**, 1268-1273.
8. T. Ami, K. Oka, K. Tsuchiya and N. Tohnai, *Angewandte Chemie*, 2022, **134**, e20222597.
9. H. Kim and M. P. Suh, *Inorganic chemistry*, 2005, **44**, 810-812.
10. K. M. E. Jones, A. H. Mahmoudkhani, B. D. Chandler and G. K. H. Shimizu, *CrystEngComm*, 2006, **8**, 303-305.
11. P. Metrangolo, F. Meyer, T. Pilati, D. M. Proserpio and G. Resnati, *Chem. Eur. J.*, 2007, **13**, 5765-5772.
12. D. Beaudoin, T. Maris and J. D. Wuest, *Nat. Chem.*, 2013, **5**, 830-834.